Effect of headgroup on the physicochemical properties of phospholipid bilayers in electric fields : size matters

Madrid, Elena; Horswell, Sarah L.

DOI:
10.1021/la304455d

Langmuir

Article

pubs.acs.org/Langmuir

Effect of Headgroup on the Physicochemical Properties of Phospholipid Bilayers in Electric Fields: Size Matters

Elena Madrid and Sarah L. Horswell*

School of Chemistry, University of Birmingham, Edgbaston, Birmingham B15 2TT, U.K.

ABSTRACT: The effect of molecular structure on ensemble structure of phospholipid films has been investigated. Bilayers of dimyristoyl phosphatidylethanolamine (DMPE) were prepared on Au(111) electrodes using Langmuir−Blodgett and Langmuir−Schaeffer deposition. Capacitance and charge density measurements were used to investigate the adsorption behavior and barrier properties of the lipid bilayers. In situ polarization modulation infrared reflection absorption spectroscopy (PM-IRRAS) was employed to investigate the organization of the molecules within the bilayer. DMPE bilayers exhibit lower capacitance than bilayers formed from the related lipid, dimyristoyl phosphatidylcholine (DMPC). The infrared data show that these results can be explained by structural differences between the bilayers formed from each molecule. DMPE organizes into bilayers with hydrocarbon chains tilted at a smaller angle to the surface normal, which results in a thicker film. The hydrocarbon chains contain few conformational defects. Spectra in the carbonyl and phosphate stretching mode regions indicate low solvent content of DMPE films. Both of these effects combine to produce films with lower capacitance and enhanced barrier properties. The results are explained in terms of the differences in structure between the constituent molecules.

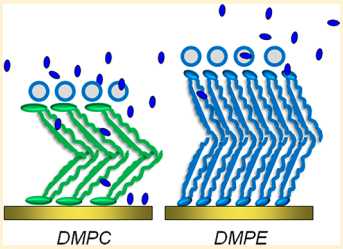

INTRODUCTION

Lipid bilayers form the basic structure of biological cell membranes, providing a highly selective barrier between the aqueous intracellular and extracellular fluids and an environment suitable for functional molecules, such as hormone receptors and proteins that control transport in and out of the cell.[1] The lipid matrix is largely composed of phospholipids, the most abundant of which in mammalian cell membranes is the class phosphatidylcholines (PC). Consequently, many studies of models of biological membranes are based on PC bilayers. Phospholipids are amphiphilic; based on a glycerol backbone, they comprise a polar headgroup and two hydrocarbon chains, as depicted in Figure 1. This general structure leads to the spontaneous assembly into a range of structures in the presence of water. The structure adopted depends on the shape of the molecule, which depends, in turn, on the size and charge of the headgroups and the lengths and degree of saturation of the hydrocarbon chains.[2] In a cell membrane, a bilayer is required where the polar headgroups face the aqueous environments inside and outside of the cell and the nonpolar, hydrophobic chains face the interior of the bilayer, thus avoiding contact with water. The molecular structure is therefore of crucial importance in determining the structure and properties of the cell membrane.

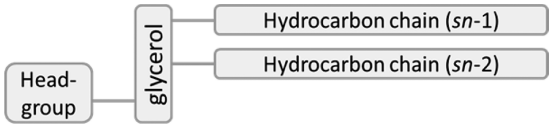

Figure 1. Schematic of general structure of phospholipid molecule.

Solid-supported lipids are attractive models for biological cell membranes because they permit the study of membrane proteins in a nondenaturing environment.[3−6] The models can be used to study the function of proteins or to incorporate functional species, such as hormone or antibody receptors, which can be used as a basis for sensing devices.[3,6−8] The use of a solid support enables the study of lipid layers with a wide range of structural probes, such as infrared spectroscopy,[9−16] sum frequency generation (SFG),[17−20] scanning tunneling microscopy (STM),[21,22] atomic force microscopy (AFM),[23−27] and reflectivity.[26,28−31] Phospholipid bilayers can be deposited on solid substrates by the fusion of small, unilamellar vesicles (SUVs)[9−11,23,29−33] or by Langmuir−Blodgett techniques.[12,13,15,34,35] The former method can sometimes facilitate more easily the inclusion of membrane peptides, but the latter allows more control over film structure and packing and tends to result in better organized films. In the present study, Langmuir−Blodgett (LB) deposition was employed for deposition of the first monolayer onto a Au(111) surface, followed by Langmuir−Schaefer (LS) deposition for the second monolayer.

A further degree of complexity to consider in the study of biomimetic lipid films is the fact that lipids and membrane proteins are frequently exposed to static electric fields, which can arise from ion gradients and/or membrane asymmetry. The magnitude of the field can vary up to an order of 10^7−10^8 V m^{-1} [9−13,29,30,36] and can cause structural rearrangements within the membranes as a result of the interactions of monopoles and dipoles with the field. When an electric field exceeds this

Received: November 8, 2012
Revised: January 2, 2013
Published: January 18, 2013

   dx.doi.org/10.1021/la304455d | *Langmuir* 2013, 29, 1695−1708

magnitude, the membrane can break down. Consequently, it would be advantageous to study lipid layers (and any incorporated membrane functional species) in this type of environment, both to mimic the natural environment and to improve understanding of electroporation, a process that is of fundamental interest and that can be exploited in gene therapy and drug delivery.[37,38] Studies of macroscopic properties, such as membrane capacitance[39−41] and conductivity,[40,42] can provide useful information on stability and membrane integrity in the presence of applied electric fields. Structural information can be inferred from such measurements but direct, molecular level information cannot be acquired.[13]

Similarly, much work has been carried out on Hg-supported lipid monolayers,[6,43−59] in which a continuously tunable electric field across the lipid monolayer can be generated by holding the Hg substrate at an electrical potential relative to an external reference electrode. Measurements such as differential capacitance, ac impedance, and coulometry can provide information on monolayer permeability (in the presence and absence of ion channel-forming peptides) and have been used to calculate surface dipoles of lipid monolayers. Capacitance and, more generally, impedance measurements can also shed light on phase transitions between different states of the film as the applied field is varied. An ideal scenario would be the simultaneous acquisition of molecular level structural information as the applied electrode potential is varied. Hg is a useful substrate in that, as a liquid, it has a smooth surface, which induces very few defects into the supported lipid layer.[60] However, it is difficult to carry out structural (e.g., spectroscopic or imaging) investigations on Hg, although some reports utilizing light fluorescent imaging[61] and X-ray reflectometry[62] have been reported. Au(111) is an alternative substrate for in situ structural investigations of lipid layers. It has a low corrugation potential for a solid substrate, is thermodynamically stable, is relatively unreactive, and has a wide potential window within which adsorption phenomena and phase transitions can be easily studied.[60] It is slightly less hydrophobic than Hg, allowing facile formation of a bilayer where headgroups face the metal and the solution phases. Added to this, it is a convenient substrate for structural studies, such as infrared spectroscopy, atomic force microscopy, reflectivity measurements, etc.[60]

Detailed in situ structural studies of phospholipid layers supported on Au(111) electrodes have been recently reviewed by Lipkowski.[60] These studies have revealed a wealth of information concerning the effect of static electric field on the structure and packing of the lipid molecules within the bilayer. Dimyristoyl phosphatidylcholine (DMPC)-based bilayers were found to be directly adsorbed on the Au(111) surface at low charge densities ($\pm 10\ \mu C\ cm^{-2}$), and at greater charge densities (hence stronger electric fields), the bilayers were found to be separated from the surface by a ∼10 Å water cushion.[29,30] The transition between these states seems to involve the ingress of solvent through the bilayer, which can also be observed by studying the ester C═O stretches in IR spectra.[9−11,13] The DMPC molecules' hydrocarbon chains were found to be more tilted at low charge densities (when directly adsorbed) than at higher charge densities (when supported on water),[9−13] in keeping with the film thicknesses determined from neutron reflectivity[29,30] and AFM[27] measurements. The inclusion of cholesterol modifies the fluidity and, consequently, electrical properties of the DMPC films.[60] The incorporation of a peptide has also been studied;[22] however, few studies have been made of non-PC-based lipid bilayers under potential control. Given the wide variety of lipids found in nature, it is necessary also to study structures formed by other lipids and to investigate their response to static electric fields, especially since particular lipids have been implicated in both binding of molecules to cell membranes and in protein function.[1] In this way, we aim to gain an understanding of why there is such a variety of lipid types in natural cell membranes.

The purpose of the present study was to investigate the influence of molecular structure on ensemble structure and properties, with a view to deepening our understanding of the role played by different types of phospholipid in cell membranes. The focus of the study was the effect of the headgroup size on packing of molecules within a lipid bilayer and, in turn, how the properties of the bilayer were affected. The molecule selected for the study was dimyristoyl phosphatidylethanolamine (DMPE), which has the same acyl chains as DMPC. Phosphatidylethanolamines (PE) are commonly found on the inner leaflet of mammalian cell membranes, whereas phosphatidylcholines (PC) are the dominant component of the outer leaflet.[1,63] The two structures are illustrated in Figure 2.

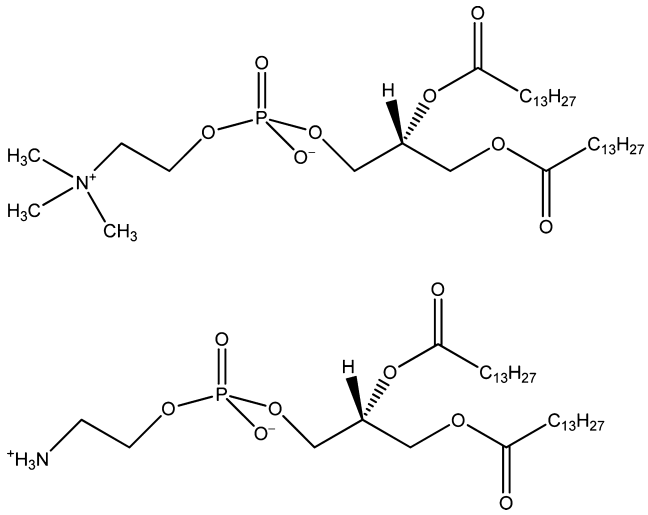

Figure 2. Top: Structure of dimyristoyl phosphatidylcholine (DMPC). Bottom: Structure of dimyristoyl phosphatidylethanolamine (DMPE).

DMPE and DMPC possess one difference: the nitrogen atom of the PE headgroup is bound to three hydrogen atoms, whereas the nitrogen atom of the PC headgroup is bound to three methyl groups. This has two consequences: the PE molecule headgroup is considerably smaller than that of PC (38 $Å^2$ compared with 50 $Å^2$),[63] leading to a roughly cylindrical shape for DMPE, and the PE molecules can interact directly with one another via hydrogen bonding.[64] PC molecules can interact indirectly via hydrogen bonding with water molecules. We show that these factors lead to a highly organized, closely packed, and slightly thicker film, which contains less solvent and has enhanced barrier properties when compared with DMPC. While infrared spectra of PE and PC dispersions in solution have previously been compared, this is the first example, to our knowledge, where infrared spectroscopy has been used to show how structure determines lipid bilayer properties and response to electric fields.

dx.doi.org/10.1021/la304455d | *Langmuir* 2013, 29, 1695−1708

EXPERIMENTAL SECTION

Materials. Dimyristoyl phosphatidylethanolamine (DMPE) and perdeuterated DMPE-d_{54} (DMPE-*d*) were purchased from Avanti Polar Lipids and used without further purification. Chloroform and methanol were HPLC grade and purchased from Sigma Aldrich. Deuterated methanol was obtained from Sigma Aldrich. Sodium fluoride (Suprapur grade, 99.99%, VWR) was used to make 0.1 M aqueous solutions. All water used for cleaning and for measurements was purified with a tandem Elix−Milli-Q Gradient A10 system (resistivity > 18 MΩ cm, TOC < 5 ppb, Millipore). All glassware was cleaned by heating in a 1:1 mixture of concentrated sulfuric and nitric acids for at least 1 h, followed by rinsing with copious quantities of ultrapure water and soaking in ultrapure water before use. Nonglass parts were cleaned with a 1:1 mixture of hydrogen peroxide and ammonia for several hours, rinsed thoroughly with ultrapure water, and soaked in ultrapure water to remove residual cleaning solution. The components of the infrared spectroelectrochemical cell were dried in an oven before use.

Electrochemical Measurements. A standard three-electrode cell was employed for differential capacitance and chronocoulometry experiments. The reference electrode was a saturated calomel electrode (SCE), contained in saturated potassium chloride solution and connected to the cell via a salt bridge. (However, since the reference electrode used in the spectroelectrochemical cell was a Ag|AgCl|3 M KCl electrode, all potentials quoted in this paper will be with respect to the Ag|AgCl electrode.) The counter electrode was a gold coil (99.999%, Alfa Aesar) and was prepared by flame annealing in a Bunsen flame and quenching with ultrapure water. The working electrode was a Au(111) single crystal (99.999% purity, orientation <0.5°, Mateck), prepared by flame annealing and rinsing with ultrapure water as described in ref 65. The electrode was transferred to the electrochemical cell with a drop of ultrapure water to reduce contamination. Once the electrochemical response of the clean surface had been checked, a bilayer of lipids was deposited and the electrode was returned to the cell.

Electrochemical measurements were carried out with a HEKA PGSTAT590 instrument and data were acquired with a PC equipped with a data acquisition board (M-series, National Instruments) and BNC block. Data acquisition software was kindly provided by Dr. Alexei Pinheiro (Universidade Tecnologica Federal do Parana, Londrina, Brazil). The software also controlled the potential applied by the potentiostat for chronocoulometry measurements. A waveform similar to that reported by Lipkowski et al. was employed for these measurements.[13] The potential was held at a base potential of −0.06 V (determined from differential capacitance measurements as a region of stability for the bilayer) for 60 s and then stepped to the potential of interest and held for 3 min to allow equilibrium to be reached. It was then stepped briefly to a potential sufficiently negative to desorb the molecules (determined from differential capacitance curves as −1.01 V) for 0.15 s, during which time a current transient was recorded, and returned to the base potential. This was repeated for a series of potentials with a step size of 50 mV and moving in the cathodic direction from 0.36 V vs SCE. For differential capacitance measurements, a dual-channel DSP 7265 lock-in amplifier (Ametek) was used to apply a 5 mV amplitude, 20 Hz frequency ac signal on top of a 5 mV s^{-1} potential sweep and to resolve the in-phase and quadrature components of the ac current response.

Langmuir Trough Measurements. A Teflon trough manufactured by Nima and equipped with a Delrin barrier and a dipper was used for Langmuir deposition of Y-type bilayers on Au surfaces. Thirty milliliters of a 1 mg mL^{-1} solution of DMPE (or DMPE-*d*) was deposited onto a clean water/air interface and allowed to equilibrate. Isotherms were recorded with a barrier speed of 25 cm^2 s^{-1}. For Langmuir deposition, the clean Au substrate (preparation described above) was placed below the surface of the water before the lipid monolayer was deposited onto the water surface. Figure 3 shows the pressure−area isotherm recorded for a DMPE monolayer at the air|water interface. The shape of the isotherm is in agreement with literature reports.[66] The isotherm shows liquid expanded (L_e), liquid condensed (L_c), and solid (S) phases, with the phase transition between the L_e and L_c phases at a pressure of ca. 5 mN m^{-1}; this portion of the isotherm can be extrapolated back to give a limiting molecular area of ∼38 $Å^2$.

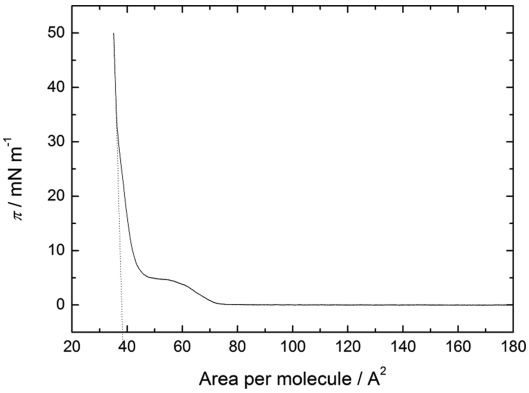

Figure 3. Pressure−area isotherm for a DMPE monolayer on a water subphase. Barrier speed 25 cm^2 s^{-1}.

The monolayer was compressed to a target pressure of 50 mN m^{-1} (which corresponds approximately to the limiting molecular area) and allowed to stabilize, after which the substrate was raised through the interface at a rate of 2 mm min^{-1} and dried in argon for 30 min. A Langmuir−Schaeffer deposition was then performed, also at 50 mN m^{-1} and a dipper speed of 2 mm min^{-1}, to afford a bilayer on the Au surface with the tail groups of the two leaflets of the bilayer pointing inward toward each other and the headgroups facing outward (a Y-type bilayer).

Infrared Measurements. PM-IRRAS measurements were carried out with a Bruker Vertex80v spectrometer with an external modified PMA50 module comprising a photoelastic modulator (PEM-100, Hinds Instruments) with a ZnSe 50 kHz optical head and synchronous sampling demodulator (GWC Technologies). Data were collected at a resolution of 2 cm^{-1} with a liquid N_2-cooled MCT-A detector. A custom-built cell was used for the measurements: the window was a BaF_2 equilateral prism (Crystran); the working electrode, on which the bilayer was deposited, was a Au(111) crystal (99.999% purity, orientation <0.5°, Mateck); the counter electrode was a concentrically wound gold wire (99.999%, Alfa Aesar); and the reference electrode was a Ag|AgCl|3 M KCl reference electrode (BASi). Three spectral regions were investigated: the C−H stretching region, the C═O stretching region, and the phosphate stretching region. The electrolyte used in the cell was 0.1 M NaF (Suprapur grade, Merck) in either ultrapure water (for the phosphate stretching region) or in deuterium oxide (for the C−H and C═O stretching regions). (Use of NaF as supporting electrolyte suppresses dissolution of the BaF_2 window.) The measurements were carried out with the PEM set for half-wave retardation at 2900 cm^{-1} for the C−H stretching region, at 1600 cm^{-1} for the C═O stretching region, and at 1100 cm^{-1} for the phosphate stretching region. The angles of incidence were selected to optimize signal using the values calculated by Zamlynny.[67] For the C−H stretching region, the angle of incidence was 51.4° and the thickness of electrolyte between the window and the Au electrode was 1.9 μm. For the C═O stretching region, the angle of incidence was 61° and the thickness of electrolyte between the window and the Au electrode was 3.6 μm. For the phosphate stretching region, the angle of incidence was 57° and the thickness of electrolyte between the window and the Au electrode was 2.1 μm. The thicknesses were calculated by comparing reflectivity spectra with the theoretical reflectivity spectra simulated for the cell configuration.[68] This procedure was carried out with "Fresnel 1" software kindly provided by Prof. V. Zamlynny (Acadia University, Nova Scotia, Canada).[69]

The demodulation technique developed by Corn et al.[70,71] was employed, following which a modification of the method described by Buffeteau et al.[72] was used to correct the intensity average and difference signals for the response of the PEM. These modifications

dx.doi.org/10.1021/la304455d | Langmuir 2013, 29, 1695−1708

have been described in detail by Lipkowski et al., along with the method employed for spline interpolation to background-correct the resulting spectra.[73] The background-corrected spectrum plots ΔS, which is related to the absorbance of the adsorbed molecules according to

$$\Delta S = \frac{2(I_s - I_p)}{I_s + I_p} \approx 2.3\Gamma\varepsilon = 2.3A \quad (1)$$

where Γ is the surface concentration of the adsorbed species, ε is the molar absorption coefficient of the adsorbed species, and A is its absorbance.[73] Separate transmission IR experiments were carried out in a specially designed liquid cell comprising BaF_2 windows separated by a 10 μm Teflon spacer. DMPE is not soluble in water or in chloroform alone; therefore, deuterated methanol (CD_3OD) had to be added to the chloroform solvent (10% v/v) and a little sodium hydroxide to the aqueous solvent to create a dispersion of randomly organized molecules. The transmission spectra were used to calculate isotropic optical constants of DMPE in chloroform and H_2O or D_2O, using software provided by Zamlynny.[69] These optical constants were used to simulate PM-IRRA spectra of randomly oriented molecules for the cell configurations used in each of the PM-IRRAS measurements, which were subsequently used for calculation of tilt angles of transition dipole moments with respect to the surface normal. Simulations were performed for DMPE films of thickness ranging from 5.5 nm (thickness of DMPC films[13]) to 6.0 nm (the expected limit for upright chains). Hydrocarbon chain tilt angles proved consistent with a 5.7 nm film and the simulated spectra reported in this work correspond to that thickness of DMPE bilayer.

RESULTS AND DISCUSSION

Electrochemical Results. Figure 4 shows the differential capacity recorded for a Au(111) electrode coated with a bilayer

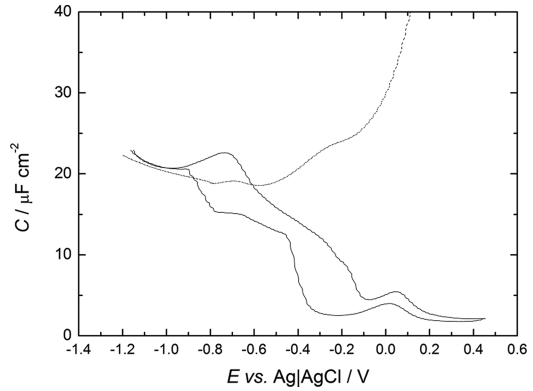

Figure 4. Differential capacity curve for a Au(111) electrode in 0.1 M NaF. Dotted line, bare Au; solid line, Au coated in a bilayer of DMPE molecules. Potential sweep rate 5 mV s^{-1}, ac frequency 20 Hz, ac amplitude 5 mV.

of DMPE molecules. The curve merges with that of the clean Au(111) substrate at potentials negative of −0.91 V, indicating that the molecules are desorbed from the surface at these potentials. On the positive sweep, a peak in capacity is observed at −0.74 V, followed by a drop in capacity. A low capacity (ca. 2.5 μF cm^{-2}) is maintained until the positive limit of the potential sweep. The negative direction exhibits slightly lower capacities: a minimum of 2.2 μF cm^{-2} is attained on this sweep. Sweeping negative, a sharp increase in capacity is seen at −0.4 V. The observed hysteresis of this phase transition may arise from slow kinetics. The minimum capacity observed (2−3 μF cm^{-2}) is lower than that reported for DMPC films formed from vesicles (~8 μF cm^{-2})[11] but higher than that expected for a bilayer on Hg. The differential capacity of a monolayer of phospholipid on Hg electrodes is ~1.6 μF cm^{-2},[6] which means that of a bilayer can be expected to be ~0.8 μF cm^{-2}. If the bilayer-coated electrode can be modeled as a simple Helmholtz capacitor, a lower capacity could be explained as a larger distance between the metal surface and the outer Helmholtz plane (distance between the capacitor "plates"), which would imply that the DMPE bilayer is thicker than a DMPC bilayer. Alternatively, the lower capacity observed for DMPE could be explained by a lower average permittivity of the DMPE bilayer, which would indicate that these films contain less water than similar DMPC films and more water than films on Hg electrodes. Hg has a perfectly smooth surface, whereas even a (111) surface of Au would be expected to have some defects, which could result in some defects in the lipid film. The infrared experiments described below were carried out to shed some light on whether the DMPE films were thicker or contained less solvent than DMPC films or both.

An estimate for the coverage, θ, of the Au(111) by the film can be calculated from

$$\theta = \frac{C_0 - C}{C_0 - C_1} \quad (2)$$

where C_0, C_1, and C are the capacities of the electrode surface covered with no film and the film without and with the defects, respectively.[74] At $E \sim 200$ mV, the capacity C_0 is equal to 35 μF cm^{-2}. The estimated coverage by DMPE of the surface film is thus approximately equal to 95% (compared with ca. 83% for DMPC films at lowest capacity). A significant difference between the differential capacity of DMPE-coated Au(111) and DMPC-coated Au(111) is in the positive potential region: a rise in capacity has been reported for DMPC as the metal becomes more positively charged,[9,11,13] which may be related to the onset of desorption positive of the potential of zero charge (pzc). The capacity curves for DMPE films in Figure 4 do not display this rise. The difference may result from differing methods of film preparation (the DMPC data were recorded for films produced by vesicle fusion) but mixed DMPE:DMPS (9:1) films formed on Au(111) by vesicle fusion also do not exhibit a rise in capacity.[31] Possibly DMPE films are more stable, at least kinetically, than DMPC films at these potentials.

The surface charge density obtained from chronocoulometric measurements, σ_M, are shown as a function of applied potential in Figure 5 for a bilayer-coated Au(111) surface and for a bare Au(111) surface. The curve for the DMPE-coated surface displays similar features to that reported for DMPC bilayers, with a step at −0.95 V indicating adsorption and another at −0.55 V indicating a phase transition to another adsorbed state. These two states for DMPC films were previously reported to consist of a bilayer supported on a water cushion (at negative charge densities) and a bilayer directly adsorbed on the Au surface (at the less negative charge densities).[29,30] DMPE appears to exhibit similar behavior to DMPC, although the slope of the curve in the less negative potential range is shallower, which mirrors the differential capacity data: a smaller σ_M−E slope indicates lower interfacial capacity.

The surface pressure, π, is a quantitative indication of the degree of adsorption. It can be evaluated from

$$\pi = \gamma_0 - \gamma = \int_{E=-1.01V}^{E} \sigma_M \, dE - \int_{E=-1.01V}^{E} \sigma_{M_0} \, dE \quad (3)$$

dx.doi.org/10.1021/la304455d | Langmuir 2013, 29, 1695−1708

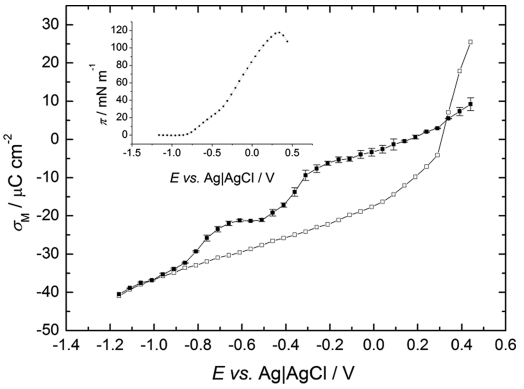

Figure 5. Plot of charge density of Au(111) in 0.1 M NaF as a function of applied electrode potential. Open squares, bare Au; filled squares, Au coated in a bilayer of DMPE molecules. Inset: Surface pressure vs applied potential, determined from the charge density plots.

where γ_0 and γ are the specific surface energies and σ_{M_0} and σ_M are the charge densities in the absence and presence of the bilayer, respectively.[75] The surface pressure for DMPE is plotted in the inset to Figure 5. A classic bell-shaped curve is obtained, displaying a maximum at the pzc. This indicates that there is a maximum in adsorption at the pzc, which is typical for the adsorption of electrically neutral molecules. The charge density range corresponding to the "adsorbed" state is ±10 μC cm^{-2}. This is similar to the range reported by Lipkowski et al. for DMPC bilayers,[13] suggesting that the range of electric field strength within which the bilayers are stable is similar.

The point at which the charge density curve for the lipid-coated surface crosses the abscissa is different from that of the base electrolyte curve; i.e., the pzc is shifted in the presence of the bilayer. This shift is (within error; the step sizes are 50 mV) identical for DMPE- and DMPC-coated electrodes. The shift can be understood as relating to an asymmetry in the charge distribution across the bilayer, where a difference in dipole orientation between the two films gives rise to a small overall dipole moment normal to the surface.[13] The shift in the pzc is given by[13,75]

$$E_N = \Gamma(\mu^{org} - n\mu^w)/\varepsilon \quad (4)$$

where E_N is the shift in the pzc, Γ is the Gibbs excess, μ^{org} is the normal component of the dipole of the phospholipids, μ^w is the normal component of the dipole of the water molecules displaced by the phospholipid molecules, n is the number of water molecules displaced by a phospholipid molecule, and ε is the permittivity.[13] μ^w is expected to be small and negative at the pzc because the water molecules should be oriented with the oxygen atoms toward the surface.[13] The results in Figure 5 suggest that the orientation of the headgroups in the DMPE film are likely to be similar to that in DMPC films.

PM-IRRAS Measurements. *Hydrocarbon Chain Vibrational Modes.* Figure 6 presents selected PM-IRRA spectra of the C−H stretching region for DMPE bilayers on Au(111). The dotted line at the top of the figure is the spectrum calculated for a monolayer of randomly oriented molecules at the surface with D_2O as the solvent. This region contains six peaks. The methyl symmetric and antisymmetric stretching vibrations are at ∼2870 and 2960 cm^{-1}, respectively, and the methylene symmetric and antisymmetric modes occur at ∼2851 and 2918 cm^{-1}, respectively.[15,64,76−84] The other two

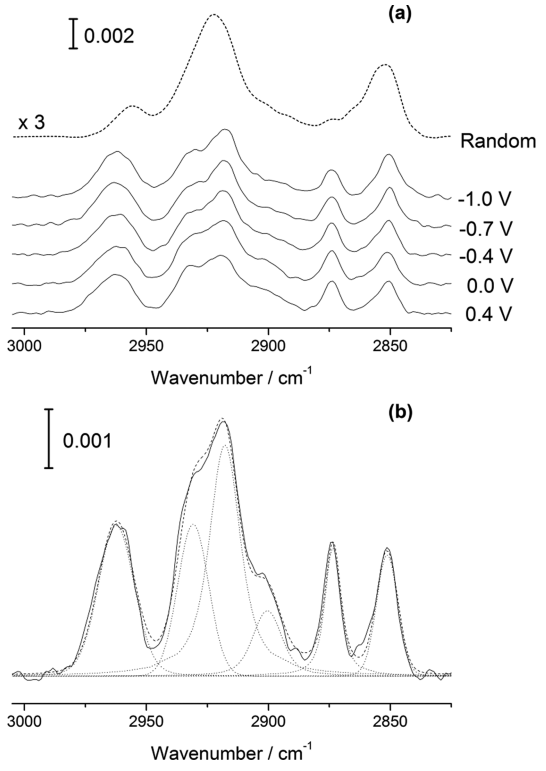

Figure 6. (a) Selected PM-IRRA spectra in the C−H stretching region at the indicated applied potentials. Dotted line: simulated spectrum of randomly oriented molecules under the same experimental conditions (scaled for clarity). (b) Example of deconvolution of the spectrum acquired at 0.0 V. Dotted lines represent each peak, the dashed line is the cumulative fit and the solid line traces the data.

modes correspond to Fermi resonances in which the methylene symmetric stretching vibrations overlap with overtones of the bending modes.[79,80,85] The spectra were analyzed further by fitting to six peaks of mixed Gaussian−Lorentzian character. An example of this fitting is shown in Figure 6b.

The spectra are generally similar to those reported for DMPC bilayers on Au(111) electrodes, but there are some differences. The relative intensities of the methylene modes (compared with the methyl vibrations and Fermi resonances) are smaller than for DMPC, which suggests a less tilted orientation of the hydrocarbon chains. The positions of the methylene stretching modes are at lower wavenumber than observed for DMPC bilayers under similar conditions.[9−13] The peak position provides an indication of the number of gauche conformers in the hydrocarbon chains, with lower wavenumbers observed at lower temperatures, where phospholipids are in the gel phase, and higher wavenumbers observed for lipids in a liquid crystalline phase at higher temperatures.[64,77−79,82] The band positions observed in Figure 6 show that the DMPE bilayer is in the gel phase. The average position over the potential range for the CH_2 symmetric stretch is 2851.5 cm^{-1} and there is a slight rise of ca. 0.5 cm^{-1} as the potential is made more positive. The antisymmetric stretching mode band changes less and averages at 2918.5 cm^{-1}. The lower wavenumber for DMPE compared with DMPC means that DMPE molecules contain, on average, fewer gauche conformers than DMPC molecules. This is consistent with differences in reported spectra comparing DPPE (dipalmitoyl phosphatidylethanolamine) with DPPC (dipalmitoyl phosphatidylcholine): the band centers for these modes in DPPC are at

dx.doi.org/10.1021/la304455d | Langmuir 2013, 29, 1695−1708

lower wavenumber than those of DPPE.[77] As those lipids were heated through the gel−liquid crystal phase transition, a sharp change in band center was observed because molecules in the liquid crystalline phase have, on average, more gauche conformers than those in the gel phase. This transition occurs at higher temperatures for DPPE than for DPPC.[77] Similarly, the chain-melting transition temperature of DMPE (50.4 °C in ref 76, 49 °C in ref 64) is higher than that of DMPC [23.6 °C in ref 64, 24.4 °C (in D_2O) in ref 86]. Hence, the DMPE film would be expected to be in the gel phase at the temperatures used in this work, whereas DMPC is in the ripple phase.[11−13,21,22] The full width half maxima (fwhm) observed for DMPE bilayers is less than those observed for DMPC bilayers, suggesting low mobility or a higher degree of ordering[76] and thus relatively tight packing. The peak positions do not change significantly as the charge on the Au surface is varied, in contrast to the case of DMPC and DOPC, where a change was observed as the bilayer lifted from the surface.[9−13] The fwhm increase slightly as the potential is made more positive, suggesting a small increase in mobility for the molecules that are directly adsorbed on the surface, in contrast with DMPC LB−LS layers, where mobility decreased slightly for adsorbed molecules.[13]

The observations made for the band intensities can be quantified following the approach of Zamlynny and Lipkowski.[73] The absorbance is related to the angle made by the transition dipole and the surface normal by[73,87]

$$\int A \, d\nu \; \alpha \, |\boldsymbol{\mu}\cdot\mathbf{E}|^2 = |\mu|^2 \langle E \rangle^2 \cos^2 \theta \tag{5}$$

where A is the absorbance, $\boldsymbol{\mu}$ is the dipole moment, $\boldsymbol{E}$ is the electric field, and θ is the angle between the transition dipole and the surface normal. By comparing the integrated band intensity with that expected for randomly oriented molecules, it is possible to calculate the angle between the transition dipole and the surface normal using[73,88,89]

$$\cos^2 \theta = \frac{1}{3} \frac{\int_E A \, d\nu}{\int_{\text{random}} A \, d\nu} \tag{6}$$

Optical constants were used to calculate the spectra of randomly oriented molecules at the surface (shown as the dotted line in Figure 6). By comparing the experimentally obtained integral peak intensities with those of the theoretical spectra of randomly oriented molecules, using eq 6, it is possible to calculate the tilt angle of the transition dipoles of each of the methylene stretching modes with respect to the surface normal. From these, the tilt angle of the hydrocarbon chains can be calculated using eq 7.[90]

$$\cos^2 \theta_s + \cos^2 \theta_{as} + \cos^2 \theta_{chain} = 1 \tag{7}$$

Figure 7 plots the tilt angles of the methylene stretching transition dipoles and the corresponding tilt angles of the hydrocarbon chains (with respect to the surface normal) as a function of applied potential. The cartoon indicates the directions of the transition dipoles relative to the hydrocarbon chain. It can be seen that the orientation of the chains changes little with applied potential. The value of the tilt angle for DMPE chains is smaller than that reported for DMPC LB−LS films:[12,13] 17° compared with 20°−24°.

The differences in the behavior of DMPE compared with DMPC can be rationalized by considering molecular geometry and packing arguments. The cross-sectional area of an all-trans

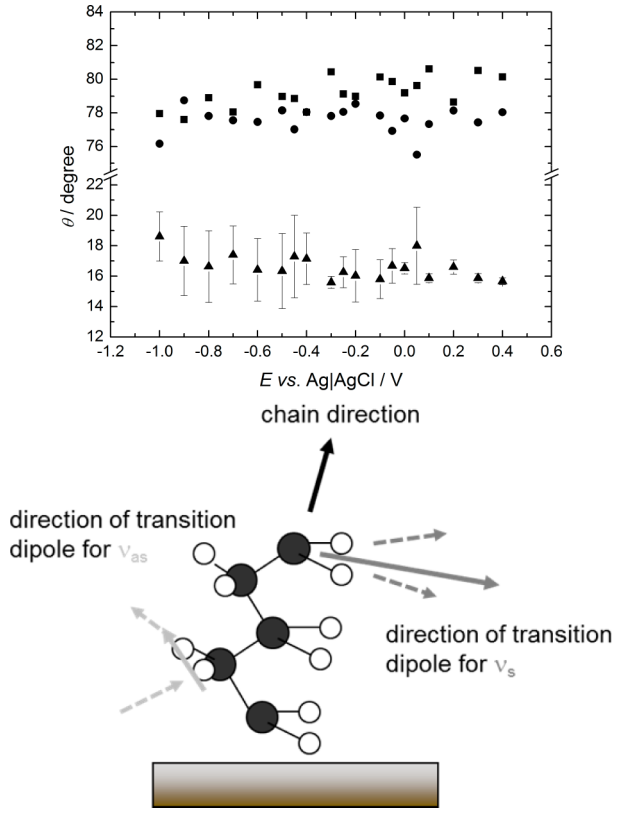

Figure 7. Plot of tilt angles as a function of applied potential: squares, tilt angle of the methylene symmetric stretch transition dipole moment; circles, tilt angle of the methylene antisymmetric stretch transition dipole moment; triangles, tilt angle of the hydrocarbon chain. Error bars indicate standard deviation between three data sets (note that the error introduced during background correction is on the order of 4°−5°). The cartoon shows the relative directions of the transition dipole moments and hydrocarbon chain backbone.

hydrocarbon chain is 18.6 Å^2,[91] so that of two all-trans hydrocarbon chains in a lipid can be taken to be ∼36−38 Å^2. The cross-sectional area of DMPE headgroups is 38 Å^2 [63] and that of DMPC headgroups is 50 Å^2.[63] The DMPE headgroup is thus of similar size to the cross-sectional area of the chains, which results in an almost cylindrical shape. The DMPC films reported in Lipkowski's work were transferred onto the substrate with a molecular area of 45 Å^2.[12,13] To maximize dispersion interactions, the DMPC hydrocarbon chains are forced to tilt. In contrast, the comparable size of the DMPE headgroups and chains means that the hydrocarbon chains do not have to tilt significantly to maintain strong dispersion interactions between the chains. This results in a lower hydrocarbon chain tilt angle for DMPE molecules adsorbed onto the Au surface. It is interesting to note that the difference in chain tilt angle for adsorbed DMPC and DMPE bilayers on Au(111) is similar to that determined by Fringeli for DPPC and DPPE films on Ge substrates (the latter determined from the CH_2 wagging mode progression).[92]

Information on chain tilt and packing arrangement of molecules can also be derived by examining the CH_2 bending mode, located at ∼1450 cm^{-1}.[9−11,13] Unfortunately, while just visible, this band was very weak and rather noisy in our spectra. For this reason, we decided not to analyze that region of the spectrum because the error in background subtraction and peak fitting would be too large.

dx.doi.org/10.1021/la304455d | Langmuir 2013, 29, 1695−1708

Figure 8 shows spectra acquired in the lower wavenumber region, where the phosphate stretching modes are found. A

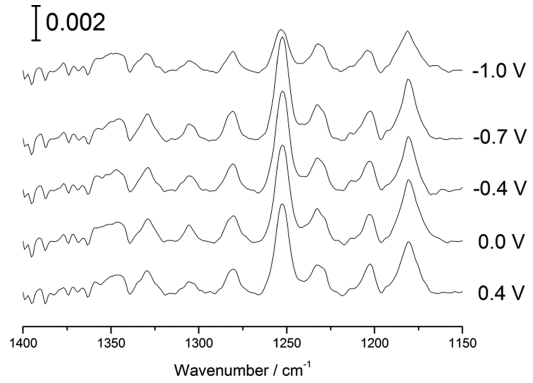

Figure 8. Selected PM-IRRA spectra of a DMPE bilayer on Au(111) in H_2O in the low wavenumber region.

number of additional peaks are present in Figure 8, reminiscent of CH_2 wagging mode progressions.[64,79−82,92,93] The peak positions of these modes are sensitive to chain length and ordering.[64,79,80,82,93,94] The peak positions of the bands in our spectra are consistent with the CH_2 wagging modes reported by Snyder et al. for cold samples of DMPC and DMPE.[93] The modes arise as a result of coupling between wagging motions of neighboring methylene units, and the number and intensities of bands observed can indicate the degree of planarity of the hydrocarbon chains. Snyder et al. reported that the chains for these molecules were all-trans, with the exception of a gauche conformer adjacent to the ester group in the *sn*-2 chain. A series of wagging modes has not been reported for DMPC bilayers on Au(111), which suggests that the DMPE molecules form a much more ordered film with fewer gauche conformers in the chains than DMPC, under the conditions employed in these experiments.

Wagging modes broaden and decrease in intensity as the number of gauche conformers increases and eventually disappear around the chain-melting transition[79,93,94] (if there are more gauche conformers, the result is a series of smaller segments of planarity in a chain, reducing the number of bands).[93,94] Spectra for the DMPC bilayers were recorded at temperatures relatively close to the main chain-melting transition, where the molecules were in the ripple phase. The main chain-melting transition of DMPE is much higher (49−50 °C[76] compared with 24 °C for DMPC),[64,86] and the molecules are in the gel phase (this is corroborated by the CH_2 band positions and fwhm). This would explain the presence of the wagging mode progression in our spectra but not in spectra of DMPC acquired at similar temperatures. The lower tilt angle of the hydrocarbon chains may also contribute to a greater intensity because the direction of the transition dipole moment for this motion would be expected to be along the direction of the hydrocarbon chain.

Interestingly, the band at 1252 cm^{-1} has the highest intensity, which is not observed for the phospholipids studied by Snyder et al. nor in our measurements of DMPS bilayers produced by LB−LS deposition, in which the intensities of the wagging modes are similar.[95] Snyder et al.[94] investigated the relative intensities of the wagging modes by performing normal mode calculations on methyl esters of acyl chains. These calculations showed that the higher intensity modes were at the 1370 cm^{-1} end of the progression. They concluded that electronic coupling of the nearest CH_2 units with the C═O vibration was responsible for the increase in intensity. In the case of our films, there is no alternative strong coupling of the wagging modes to explain the heightened intensity of the 1252 cm^{-1} peak, which suggests that this peak overlaps with the phosphate antisymmetric stretching mode, which is expected to be ∼1220−1260 cm^{-1},[1,76,77,82,84,92,96−98] increasing its intensity relative to the rest of the peaks in the progression. The contribution of the phosphate modes was removed in ref 93 by subtracting a spectrum acquired at higher temperatures, where the wagging modes had vanished and the phosphate modes remained. In our experiments, the temperatures needed to achieve this would result in significant evaporation of water, which is a problem for the long time scales needed to record high-quality spectra. Therefore, we decided to record spectra using DMPE with fully deuterated hydrocarbon chains (DMPE-*d*) to determine the position of the phosphate antisymmetric stretching mode, since CD_2 vibrational modes will be positioned at lower wavenumber than the corresponding CH_2 modes. These spectra (vide infra) show that the phosphate antisymmetric stretching mode makes a contribution to the 1252 cm^{-1} band observed in Figure 8, explaining the somewhat larger intensity of this peak.

Interfacial and Headgroup Regions. The phosphate group of a phospholipid gives rise to two O−P−O stretching vibrations of the nonesterified oxygen atoms: an antisymmetric and a symmetric mode. Vibrations of the other P−O[C] bonds, where the oxygen atoms are attached to the rest of the headgroup or to the glycerol moiety, are also observed in this spectral region. A range of band positions has been reported for the O−P−O vibrations for PC, PE, and PS (phosphatidylserine) lipids, normally depending on the degree of hydration.[64,76,78,82,84,96−102] The band positions for DMPC in similar experiments to ours have been reported as 1231 and 1089.5 cm^{-1} (ν_{as} and ν_s, respectively) for hydrated samples (films adsorbed at low charge densities) and 1237.5 and 1094.5 cm^{-1} for less hydrated states of the films, where the films were separated from the surface by a water cushion.[11,13] Lewis and McElhaney reported ν_{as} and ν_s positions of 1224 and 1083 cm^{-1}, respectively, for dehydrated, ordered polymorphs of DMPE, with a slightly less well-ordered polymorph giving bands at 1261, 1239, 1222, and 1090 cm^{-1}.[76] Narrow bands indicated a lack of mobility, and the lower wavenumber bands were ascribed to hydrogen bonded phosphate groups. A study of dioleoyl phosphatidylethanolamine (DOPE) as a function of relative humidity showed a sudden change for the symmetric vibrational mode from ∼1082 to 1076 cm^{-1} at a relative humidity of 50%, compared with a gradual decrease from 1093 to 1089 cm^{-1} for DPPC (dipalmitoyl phosphatidylcholine) as humidity was increased.[98] The sharpness of the change was considered to result from a phase transition between two states of different hydration; the band position is red-shifted when the phosphate group participates in hydrogen bonding.[98] Sen et al. studied the IR spectra of PE in various solvents and solvent mixtures and reported a decrease in wavenumber of the phosphate band centers in the presence of water.[97]

The phosphate O−P−O antisymmetric stretching mode is thus located in the spectral region where the methylene wagging modes are observed (vide supra), which makes it difficult to analyze. For this reason, spectra were also acquired with bilayers formed from DMPE-*d*, and selected spectra are presented in Figure 9, along with simulated spectra for

dx.doi.org/10.1021/la304455d | *Langmuir* 2013, 29, 1695−1708

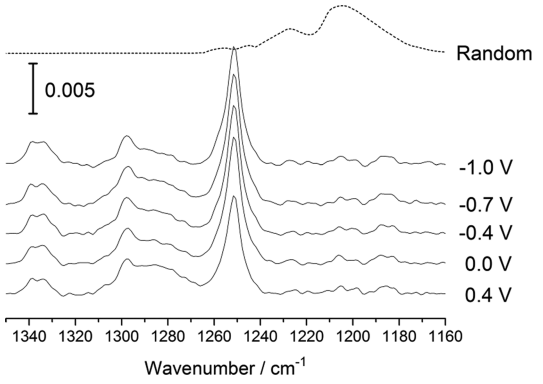

Figure 9. Selected PM-IRRA spectra of DMPE-*d* in H_2O in the low wavenumber region. Dashed line: simulation of spectra of randomly organized molecules under the same experimental conditions.

randomly oriented molecules in H_2O. (It should be noted that, in this aqueous dispersion, a significant fraction of the amine groups is deprotonated in order to enable dissolution; the higher pH may impact on the size and shape of the bands observed and the spectrum can only be used for qualitative comparison.)

A single, relatively narrow band is visible for the DMPE-*d* bilayers at 1251.6(±0.1) cm^{-1}, somewhat higher than reported for DMPC molecules adsorbed on Au(111) electrodes under similar conditions and a little higher than normally reported, for example, by Lewis and McElhaney for DMPE polymorphs. However, Binder and Pohle reported band centers of 1245 and 1248 cm^{-1} for DOPE in the presence of H_2O and 9:1 D_2O:H_2O, respectively, at controlled relative humidity.[99] The high wavenumber observed in Figure 9 indicates that the DMPE headgroups do not participate extensively in hydrogen bonding with water; the headgroups are dehydrated. They are also relatively immobilized, since the fwhm of the peak, on average 8.7(±0.2) cm^{-1}, is lower than that observed for similar DMPC films (36−38 cm^{-1}).[13] By contrast, the simulated spectrum of molecules in a hydrated environment displays a broad, red-shifted absorption, owing to extensive hydrogen bonding within the dispersion. Figure 9 also shows that the fwhm and position of the O−P−O ν_{as} mode are invariant with applied electrode potential. (Bands are also observed at 1285 and 1336 cm^{-1}; their origin is not clear, although they may be associated with deformation modes of C−H groups in the headgroup.) The C−O−C vibrational mode of the carbonyl groups is expected at ∼1170−1180 cm^{-1}.[13,92,97] This vibration is not obvious in the spectra shown in Figure 9, but a small bump is present at 1185 cm^{-1} (the spectra were rather noisy in this region). The band is expected to be weaker than observed for DMPC: the geometry of the molecule dictates that the plane of the carbonyl group should be closer to parallel to the surface for DMPE, since the hydrocarbon chains are more upright. The frequency observed is indicative of a planar geometry for the OCO group.[13,92]

Spectra in the phosphate symmetric stretching vibration region, at selected applied potentials, are presented in Figure 10a for bilayers formed from DMPE-*d* and in Figure 10b for bilayers formed from nondeuterated DMPE (DMPE-*h*). This comparison is made to ensure that conclusions about headgroup behavior drawn from spectra acquired for deuterated molecules are also applicable to nondeuterated molecules. In each case, the dashed line shows a calculated spectrum for a 5.7 nm thick film of randomly oriented

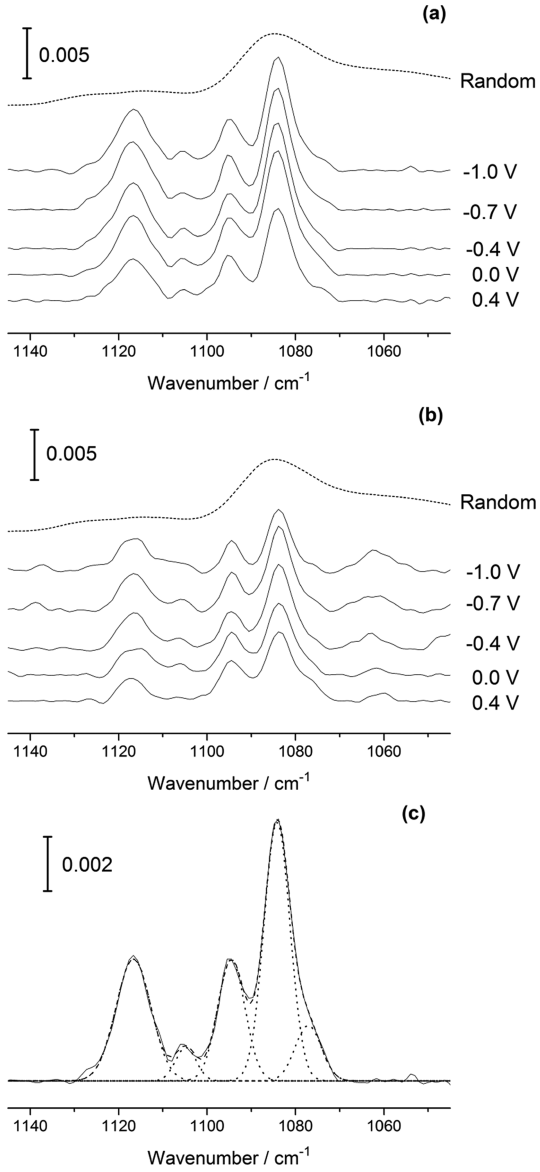

Figure 10. (a) Selected PM-IRRA spectra of DMPE-*d* in H_2O, showing the phosphate symmetric stretching mode. (b) Selected PM-IRRA spectra of DMPE-*h* in H_2O, showing the phosphate symmetric stretching mode. Dashed line in each case: simulation of spectra of randomly organized molecules under the same experimental conditions [angle of incidence, 57°; distance between electrode and BaF_2 window, 2.1 μm in (a), 2.3 μm in (b)]. (c) Example of a deconvolution into the O−P−O stretching mode and the phosphate ester stretching vibrations (spectrum in part a acquired at 0.0 V).

molecules. The spectra in Figure 10a,b are similar, each consisting of a pair of peaks at 1094.5(±0.2) and 1084.0(±0.4) cm^{-1} and a broader peak at 1116 cm^{-1}. The 1084 cm^{-1} band has a lower wavenumber tail. A deconvolution of one of the spectra in Figure 10a (that acquired at 0 V) is shown in Figure 10c. The bands at 1094.5 and 1084 cm^{-1} are likely to arise from the O−P−O symmetric stretching mode; the 1116 cm^{-1} band and the lower wavenumber tail (∼1075 cm^{-1}) are consistent with vibrations involving the esterified oxygen atoms.[10,11,13,103] The ν_s bands are narrow, much narrower than reported for DMPC, for which a single, broad band overlapping with P−O[C] modes is observed.[11,13] The corresponding band for dispersed DMPE is broader and not split. The narrow bands

dx.doi.org/10.1021/la304455d | *Langmuir* 2013, 29, 1695−1708

observed in both Figures 9 and 10 thus indicate relatively immobile headgroups. The presence of two bands for supported DMPE bilayers might indicate two environments that can be distinguished by virtue of the narrowness of the bands. Tentatively, these could be assigned to two different regions within the bilayer or to the Au-facing layer and the water-facing layer, in which case the difference in peak size might indicate different orientations of the two headgroups of the two layers. (This might, in turn, explain the presence of the small dipole moment across the bilayer observed in the electrochemical data.) On the other hand, splitting of bands arising from phosphate stretching vibrations has also been ascribed to lowering of symmetry upon complexation of metal ions to PS.[101,102] Potentially, the adsorption of the phosphate group onto the Au surface could also reduce symmetry and give rise to splitting. However, this was not observed for DMPC bilayers on Au and it is less likely that DMPE phosphate groups, which participate in stronger intermolecular interactions, would exhibit stronger adsorption on Au than DMPC. Directed hydrogen bonding interactions with adjacent amine groups might also cause splitting. However, a splitting of the ν_{as} band might also be expected if the two nonesterified oxygen atoms become inequivalent,[97] and this is not observed in our spectra.

The positions and fwhm of the phosphate group bands change little with applied potential, which is suggestive of little change in local environment for the headgroups when the bilayer passes through the phase transition observed at −0.4 V. If the phase transition involves water ingress, as was observed for DMPC-based films,[29,30] the DMPE molecules seem to interact little with the water. The 1094 cm^{-1} band changes less with applied potential than the 1084 cm^{-1} band; if the two bands were to correspond to different leaflets of the bilayer, these observations could be interpreted as a change in conformation of the headgroups of one of the leaflets. A gradual increase in band intensity of both the symmetric and antisymmetric stretching mode bands is observed between approximately 0.2 V and −0.5 V. The intensity decreases at the extreme negative potentials, where the bilayer begins to desorb from the surface, reaching a similar intensity to that observed at the most positive potentials. Figure 11a is a plot of estimated tilt angle of the ν_{as} and ν_s modes as a function of potential (the total area of the ν_s modes in each spectrum was used for the calculation). This plot should be regarded only as an estimate of tilt angle because the form of the bands is different for the simulated spectra and experimental spectra of bilayers, which means that the intensity of the band may be affected by the difference in hydrogen bonding between the dispersion of molecules and the adsorbed bilayers. Nevertheless, it is useful to plot the data in the form of tilt angle rather than as raw peak area for two reasons: (i) it facilitates comparison between data sets and estimate of error (it provides a normalization of peak area, as peak area alters with slight differences in spectroelectrochemical cell configuration between experiments), and (ii) it gives a better idea of the extent of change in tilt angle as the applied potential is varied. The bottom trace in Figure 11a shows the estimated tilt angle of the O−P−O direction, calculated from those of the two vibrational modes using eq 7, in an analogous fashion to calculation of the hydrocarbon chain tilt angle from the two mutually perpendicular modes.[10,11,13] It is interesting to note that the direction of the ν_s transition dipole has slightly higher tilt for DMPE-*h* compared with DMPE-*d*, indicating that the phosphate group has slightly

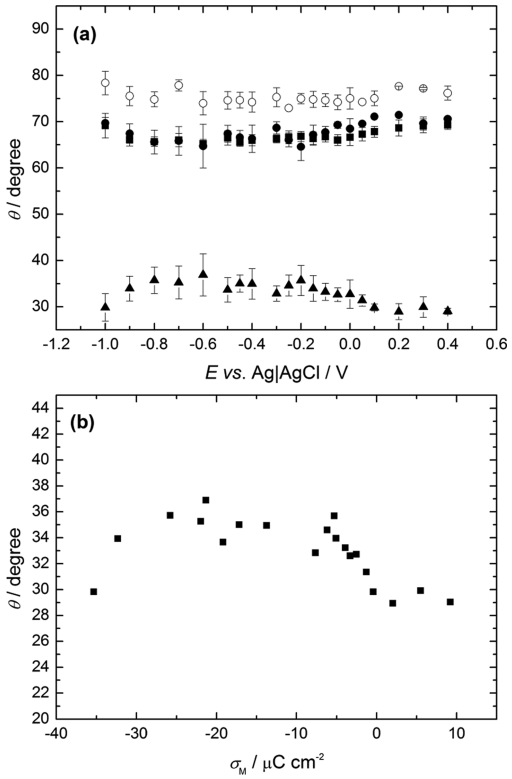

Figure 11. (a) Estimate of tilt angles from PO_2 stretching modes as a function of applied potential: filled shapes, DMPE-*d*; open shapes DMPE-*h*; circles, symmetric stretching vibration transition dipole moment; squares, antisymmetric stretching vibration transition dipole moment; triangles, tilt of the O−P−O direction with respect to the surface normal. (b) Plot of the estimated tilt angle of the O−P−O direction with respect to the surface normal as a function of charge on the metal surface.

flatter orientation for DMPE-*h*. However, the trend in behavior is similar for the two molecules and the DMPE-*d* data can be used as a guide to the general behavior of DMPE. The ν_s and ν_{as} mode transition dipole moments of DMPE-*d* have similar orientation, as has been reported for DMPC LB−LS bilayers.[13] The tilt angle of the O−P−O direction is higher than for DMPC[13] but, given that the ν_s mode for DMPE is similar to that of DMPC, it is likely that the tilt angle of the O−P−O direction in DMPE is similar to that of DMPC. Some insight into the changes in orientation of the molecules can be gained by plotting the O−P−O tilt angle as a function of charge density on the metal. Figure 11b shows that the change in absorbance occurs on changing from positive to negative charge densities. As the metal becomes negatively charged, an increase in absorbance is observed until ca. 10 $\mu C\ cm^{-2}$, which is the charge density at the onset of the phase transition observed in the chronocoulometry measurements. When the charge density exceeds ca. 30 $\mu C\ cm^{-2}$, where the bilayer finally desorbs, the absorbance decreases. Lipkowski remarked that a DMPC bilayer resting on an electrolyte cushion at negative applied potentials would experience an attenuated electric field.[29,30] Hence, the field experienced by the lipids is small in both the applied potential regions 0.2−0.4 V and −0.9 to −1.0 V. This might result in a similar orientation of the headgroup dipoles in these potential regions, explaining their similar band intensities. Unfortunately, it is not possible to construct a complete model of the orientation of headgroups because the $[-NH_3]^+$ modes

dx.doi.org/10.1021/la304455d | Langmuir 2013, 29, 1695−1708

are hidden by strong signals from the electrolyte (note that use of $[-ND_3]^+$ would simply result in exchange of deuterium with the electrolyte). Nevertheless, it is still possible to note that the headgroups respond to the electric field, although the effect this has on the orientations of the other functional groups of the molecules is small. The tight packing of the hydrocarbon chains may restrict the reorientation of molecules under the influence of an applied field, but the headgroups, particularly in the water-facing layer, may have more flexibility.

Figure 12 presents spectra in the C═O stretching region for DMPE bilayers at selected applied potentials. The phospholipid

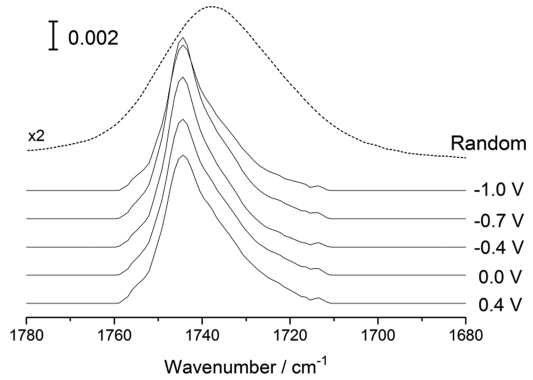

Figure 12. Selected PM-IRRA spectra in the C═O stretching region at the indicated applied potentials. Dotted line: simulated spectrum of randomly oriented molecules under the same experimental conditions (scaled for clarity).

C═O stretching band is sensitive to the environment of the interfacial region of the molecule, with a peak position at higher wavenumber indicating very little hydrogen bonding and at lower wavenumber indicating significant hydrogen bonding.[76,82,96,104,105] Often, a band is observed composed of two or three components, the relative intensities of which can give an indication of the extent of hydrogen bonding. Hence, the shape and position of this band can provide information about the hydration of this functional group.[9−13,15,76,82]

DMPE has been reported to exhibit bands composed of up to three components, depending on its form: a single band centered at ∼1740 cm^{-1} was observed for a dried sample and three bands at ∼1740, 1730, and 1720 cm^{-1} for a sample exhibiting less order.[76] It was suggested that the 1740 cm^{-1} band corresponded to non-hydrogen-bonded carbonyl groups, the 1730 cm^{-1} band corresponded to carbonyl groups hydrogen bonded with water molecules, and the 1720 cm^{-1} band was tentatively assigned to hydrogen bonding between the *sn*-2 carbonyl groups and the amine groups of neighboring molecules. Hydrated samples tended to exhibit two bands in the gel phase. DPPE has also been reported to have a low-frequency shoulder on the lower wavenumber band, which was attributed to interaction between water and the carbonyl group.[96] The spectra in Figure 12 show an asymmetric band, which may be composed of two or three. The dominant component of this band has its position at approximately 1740 cm^{-1} and the minor component is centered at approximately 1728 cm^{-1}. If the band is fitted to three components (averaging at 1744, 1733, and 1722 cm^{-1}), the quality of the fits is slightly improved. The percentage of the integrated area corresponding to the 1744 cm^{-1} band, plotted in Figure 13 at various applied potentials, is about 70−75%. This proportion would be indicative of an environment with little hydrogen bonding,

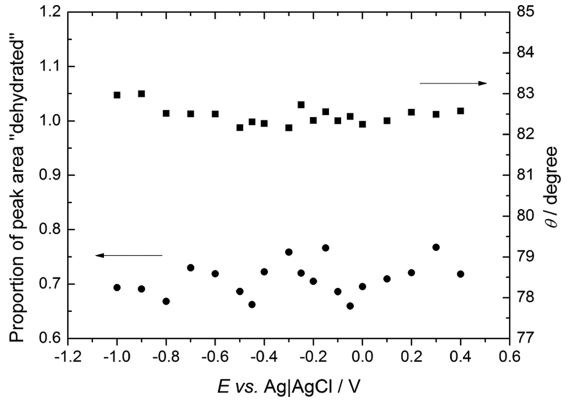

Figure 13. Circles: proportion of the total C═O band intensity taken by the 1744 cm^{-1} "dehydrated" band as a function of applied potential. Squares: C═O tilt angle as a function of applied potential.

where the DMPE molecules are predominantly in a dehydrated state. The shape of the band changes little with applied potential, although a slightly increased low wavenumber tail can be discerned at the more negative potentials (larger charge densities). Figure 13 also shows a small general trend toward lower contribution to the band from the 1744 cm^{-1} component at negative potentials. These observations suggest a small increase in hydration of DMPE molecules in this phase compared with positive of the phase transition (low charge densities) observed in the electrochemical data. The lack of hydration of the carbonyl groups observed from our spectra provides an explanation of the low capacity obtained with electrochemical measurements: a low solvent content in the bilayer is consistent with a low value of capacity.

The intensity of a given component of the C═O band could be affected by a change in hydration of the DMPE molecules or by a change in average orientation of the carbonyl groups (the *sn*-1 and *sn*-2 carbonyl groups may have different orientations). Therefore, it is only possible to estimate a change in average tilt angle of the carbonyl groups. Figure 13 also plots this estimated tilt angle as a function of potential. The tilt angle changes very little with applied potential, in contrast to DMPC.[13] A small increase in tilt angle is observed at the most negative potentials, similarly to DMPC, but in the case of DMPE the change is ca. 1°, within the error margin. The average angle, at about 82.5°, indicates a C═O group lying almost parallel to the metal surface, which is consistent with a small tilt angle of hydrocarbon chains.

Drawing together the information from different spectral regions, a model for the structure of the DMPE bilayer can be proposed to explain its electrochemical properties. Figure 14 is a cartoon comparing a DMPE film on Au(111) with a DMPC film (the latter adapted from figures in refs 13, 29, and 30). The cartoon shows schematically that the DMPE films contain less solvent than DMPC films and also offers a model for the packing of molecules that gives rise to a smaller tilt of the hydrocarbon chain from the surface normal. The outer Helmholtz plane is pushed away from the surface; this fact, combined with the lower solvent content, explains the lower capacity observed for DMPE films. The relatively tighter packing of the DMPE molecules also explains the smaller changes in molecular orientation observed as the applied electric field is strengthened.

dx.doi.org/10.1021/la304455d | *Langmuir* 2013, 29, 1695−1708

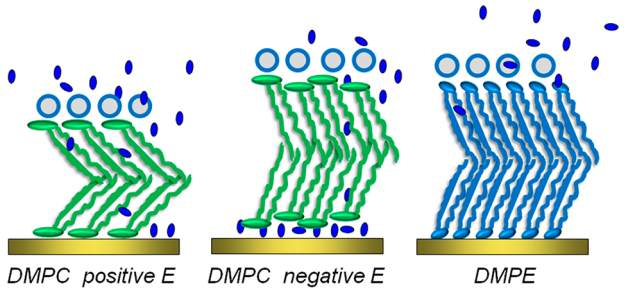

Figure 14. Schematic diagram showing suggested difference between DMPE and DMPC bilayer films on Au surfaces (DMPC adapted from refs 13, 29, 30). Circles represent solvated ions in the outer Helmholtz plane, and small ellipsoids represent water (not to scale but illustrating differences in the average solvent content of film).

CONCLUSIONS

The influence of the phospholipid molecular structure on its packing and ensemble properties is striking. By reducing the size of the headgroup such that its area is closer to that occupied by the hydrocarbon chains, it is possible to create bilayer films that have significantly enhanced electrical barrier properties. This finding can be explained by investigating the film structure and molecular organization in detail with in situ PM-IRRAS measurements. The smaller headgroup allows closer packing of molecules, with most of the molecules' chains in an all-trans conformation and oriented with the chain backbone closer to the surface normal. The tighter packing decreases film permeability to water (evident in the lack of hydrogen bonding in the glycerol part of the molecule) and the smaller tilt of the chains increases slightly bilayer thickness. These effects combine to decrease the capacitance of the bilayer. The DMPE film undergoes a phase transition similar to that previously observed for DMPC, but the PM-IRRA spectra indicate remarkably few changes in ensemble structure. Apparently, there is little difference in film organization and structure in each phase. This observation has implications for the choice of phospholipid in lipid films used as biological membrane mimics or as a matrix for sensing molecules. The fluidity of DMPE films is rather low, which may make them less suitable as mimics of biological membranes when used alone. On the other hand, the reduced permeability to water and the stability in ensemble structure over a wide range of applied electric field may be considerable advantages for creating a base film for the incorporation of other molecules to create solid-supported sensors.

AUTHOR INFORMATION

Corresponding Author

*E-mail: s.l.horswell@bham.ac.uk.

Notes

The authors declare no competing financial interest.

ACKNOWLEDGMENTS

This work was supported by EPSRC (grant number EP/D05561X/1) and by the Royal Society (Small Equipment Grant). E.M. is grateful to the School of Chemistry, University of Birmingham, for a studentship. The authors are indebted to Prof. V. Zamlynny and Prof. J. Lipkowski for helpful discussions about the experimental setup and for kindly allowing us to use the Fresnel software. The technical advice and support of Prof. T. Rayment, Mr. A. Rothin, Mr. S. Williams, and Mr. S. G. Arkless are gratefully acknowledged, as is the help of Dr. A.L.N. Pinheiro with the data acquisition software.

REFERENCES

(1) Alberts, B.; Johnson, A.; Lewis, J.; Raff, M.; Roberts, K.; Walter, P. *Mol. Biol. Cell*, 4th ed.; Taylor and Francis: London, 2002, Chapter 10.
(2) Pashley, R. M.; Karaman, M. E. *Applied Colloid Surface Chemistry*; Wiley: New York, 2004.
(3) Sackmann, E. Supported membranes: Scientific and practical applications. *Science* **1996**, *271*, 43−48.
(4) Kalb, E.; Rey, S.; Tamm, L. K. Formation of planar supported bilayers by fusion of vesicles to supported phospholipid monolayers. *Biochim. Biophys. Acta* **1992**, *1103*, 307−316.
(5) Castellana, E. T.; Cremer, P. S. Solid-supported lipid bilayers: From biophysical studies to sensor design. *Surf. Sci. Rep.* **2006**, *61*, 429−444.
(6) Guidelli, R.; Aloisi, G.; Becucci, L.; Dolfi, A.; Moncelli, M. R.; Buoninsegni, F. T. Bioelectrochemistry at metal | water interfaces. *J. Electroanal. Chem.* **2001**, *504*, 1−28.
(7) Andra, J.; Bohling, A.; Gronewold, T. M. A.; Schlecht, U.; Perpeet, M.; Gutsmann, T. Surface acoustic wave biosensor as a tool to study the interaction of antimicrobial peptides with phospholipid and lipopolysaccharide model membranes. *Langmuir* **2008**, *24*, 9148−9153.
(8) Albertorio, F.; Diaz, A. F.; Yang, T. L.; Chapa, V. A.; Kataoka, S.; Castellana, E. T.; Cremer, P. S. Fluid- and air-stable lipopolymer membranes for biosensor applications. *Langmuir* **2005**, *21*, 7476−7482.
(9) Horswell, S. L.; Zamlynny, V.; Li, H.-Q.; Merrill, A. R.; Lipkowski, J. Electrochemical and PM-IRRAS studies of potential controlled transformations of phospholipid layers on Au(111) electrodes. *Faraday. Discuss.* **2002**, *121*, 405−422.
(10) Zawisza, I.; Lachenwitzer, A.; Zamlynny, V.; Horswell, S. L.; Goddard, J. D.; Lipkowski, J. Electrochemical and photon polarization modulation infrared reflection absorption spectroscopy study of the electric field driven transformations of a phospholipid bilayer supported at a gold electrode surface. *Biophys. J.* **2003**, *86*, 4055−4075.
(11) Bin, X.; Zawisza, I.; Goddard, J. D.; Lipkowski, J. Electrochemical and PM-IRRAS studies of the effect of the static electric field on the structure of the DMPC bilayer supported at a Au(111) electrode surface. *Langmuir* **2005**, *21*, 330−347.
(12) Garcia-Araez, N.; Brosseau, C. L.; Rodriguez, P.; Lipkowski, J. Layer-by-layer PMIRRAS characterization of DMPC bilayers deposited on a Au(111) electrode surface. *Langmuir* **2006**, *22*, 10365−10371.
(13) Zawisza, I.; Bin, X.; Lipkowski, J. Potential-driven structural changes in Langmuir−Blodgett DMPC bilayers determined by in situ spectroelectrochemical PM IRRAS. *Langmuir* **2007**, *23*, 5180−5194.
(14) Zawisza, I.; Nullmeier, M.; Pust, S. E.; Boukherroub, R.; Szunerits, S.; Wittstock, G. Application of thin titanium/titanium oxide layers deposited on gold for infrared reflection absorption spectroscopy: Structural studies of lipid bilayers. *Langmuir* **2008**, *24*, 7378−7387.
(15) Dicko, A.; Bourque, H.; Pezolet, M. Study by infrared spectroscopy of the conformation of dipalmitoylphosphatidylglycerol monolayers at the air−water interface and transferred on solid substrates. *Chem. Phys. Lipids* **1998**, *96*, 125−139.
(16) Duevel, R. V.; Corn, R. M.; Liu, M. D.; Leidner, C. R. Orientation and organization in functionalized phospholipid monolayers at gold surfaces as measured by polarization modulation Fourier-transform infrared-spectroscopy. *J. Phys. Chem.* **1992**, *96*, 468−473.
(17) Liu, J.; Conboy, J. C. 1,2-Diacyl-phosphatidylcholine flip-flop measured directly by sum-frequency vibrational spectroscopy. *Biophys. J.* **2005**, *89*, 2522−2532.
(18) Liu, J.; Conboy, J. C. Direct measurement of the transbilayer movement of phospholipids by sum-frequency vibrational spectroscopy. *J. Am. Chem. Soc.* **2004**, *126*, 8376−8377.

(19) Liu, J.; Conboy, J. C. Phase transition of a single lipid bilayer measured by sum-frequency vibrational spectroscopy. *J. Am. Chem. Soc.* **2004**, *126*, 8894−8895.
(20) Chen, X.; Tang, H.; Even, M. A.; Wang, J.; Tew, G. N.; Chen, Z. Observing a molecular knife at work. *J. Am. Chem. Soc.* **2006**, *128*, 2711−2714.
(21) Xu, S.; Szymanski, G.; Lipkowski, J. Self-assembly of phospholipid molecules at a Au(111) electrode surface. *J. Am. Chem. Soc.* **2004**, *126*, 12276−12277.
(22) Sek, S.; Laredo, T.; Dutcher, J. R.; Lipkowski, J. Molecular resolution imaging of an antibiotic peptide in a lipid matrix. *J. Am. Chem. Soc.* **2009**, *131*, 6439−6444.
(23) Feng, Z. V.; Spurlin, T. A.; Gewirth, A. A. Direct visualization of asymmetric behavior in supported lipid bilayers at the gel-fluid phase transition. *Biophys. J.* **2005**, *88*, 2154−2164.
(24) Ngwa, W.; Chen, K.; Sahgal, A.; Stepanov, E. V.; Luo, W. Nanoscale mechanics of solid-supported multilayered lipid films by force measurement. *Thin Solid Films* **2008**, *516*, 5039−5045.
(25) Reviakine, I.; Brisson, A. Formation of supported phospholipid bilayers from unilamellar vesicles investigated by atomic force microscopy. *Langmuir* **2000**, *16*, 1806−1815.
(26) Koenig, B. W.; Kruger, S.; Orts, W. J.; Majkrzak, C. F.; Berk, N. F.; Silverton, J. V.; Gawrisch, K. Neutron reflectivity and atomic force microscopy studies of a lipid bilayer in water adsorbed to the surface of a silicon single crystal. *Langmuir* **1996**, *12* (5), 1343−1350.
(27) Chen, M.; Li, M.; Brosseau, C. L.; Lipkowski, J. AFM studies of the effect of temperature and electric field on the structure of a DMPC−cholesterol bilayer supported on an Au(111) electrode surface. *Langmuir* **2009**, *25*, 1028−1037.
(28) Jing, H. Y.; Hong, D. H.; Kwak, B. D.; Choi, D. J.; Shin, K.; Yu, C.-J.; Kim, J. W.; Noh, D. Y.; Seo, Y. S. X-ray reflectivity study on the structure and phase stability of mixed phospholipid multilayers. *Langmuir* **2009**, *25*, 4198−4202.
(29) Burgess, I.; Li, M.; Horswell, S. L.; Szymanski, G.; Lipkowski, J.; Majewski, J.; Satija, S. Electric field-driven transformations of a supported model biological membrane—An electrochemical and neutron reflectivity study. *Biophys. J.* **2004**, *86*, 1763−1776.
(30) Burgess, I.; Szymanski, G.; Li, M.; Horswell, S. L.; Lipkowski, J.; Majewski, J.; Satija, S. Influence of the electric field on a bio-mimetic film supported on a gold electrode. *Colloid Surf. B* **2005**, *40*, 117−122.
(31) Hillman, A. R.; Ryder, K. S.; Madrid, E.; Burley, A. W.; Wiltshire, R. J.; Merotra, J.; Grau, M.; Horswell, S. L.; Glidle, A.; Dalgliesh, R. M.; Hughes, A.; Cubitt, R.; Wildes, A. Structure and dynamics of phospholipid bilayer films under electrochemical control. *Faraday Discuss.* **2010**, *145*, 357−379.
(32) Xie, A. F.; Yamada, R.; Gewirth, A. A.; Granick, S. Materials science of the gel to fluid phase transition in a supported phospholipid bilayer. *Phys. Rev. Lett.* **2002**, *89*, 246103.
(33) Leonenko, Z. V.; Carnini, A.; Cramb, D. T. Supported planar bilayer formation by vesicle fusion: the interaction of phospholipid vesicles with surfaces and the effect of gramicidin on bilayer properties using atomic force microscopy. *Biochim. Biophys. Acta* **2000**, *1509*, 131−147.
(34) Tamm, L. K.; McConnell, H. M. Supported phospholipid-bilayers. *Biophys. J.* **1985**, *47*, 105−113.
(35) Crane, J. M.; Tamm, L. K. Role of cholesterol in the formation and nature of lipid rafts in planar and spherical model membranes. *Biophys. J.* **2004**, *86*, 2965−2979.
(36) Tsong, T. Y.; Astumian, R. D. Electroconformational coupling−How membrane-bound ATPase transduces energy from dynamic electric-fields. *Annu. Rev. Physiol.* **1988**, *50*, 273−290.
(37) Barnett, A.; Weaver, J. C. Electroporation: A unified, quantitative theory of reversible electrical breakdown and mechanical rupture in artificial planar bilayer membranes. *J. Electroanal. Chem. Bioelectrochem. Bioenerg.* **1991**, *25*, 163−182.
(38) Gehl, J. Electroporation: Theory and methods, perspectives for drug delivery, gene therapy and research. *Acta Physiol. Scand.* **2003**, *177*, 437−447.
(39) Bamberg, E.; Benz, R. Voltage-induced thickness changes of lipid bilayer membranes and effect of an electric-field on gramicidin A channel formation. *Biochim. Biophys. Acta* **1976**, *426*, 570−580.
(40) Florin, E. L.; Gaub, H. E. Painted supported lipid membranes. *Biophys. J.* **1993**, *64*, 375−383.
(41) Cohen, R.; Schmitt, B. M.; Atlas, D. Molecular identification and reconstitution of depolarization-induced exocytosis monitored by membrane capacitance. *Biophys. J.* **2005**, *89*, 4364−4373.
(42) Krishna, G.; Schulte, J.; Cornell, B. A.; Pace, R.; Wieczorek, L.; Osman, P. D. Tethered bilayer membranes containing ionic reservoirs: The interfacial capacitance. *Langmuir* **2001**, *17*, 4858−4866.
(43) Miller, I. R. In *Topics in Bioelectrochemistry and Bioenergetics*; Milazzo, G., Ed.; Wiley: Chichester, UK, 1981; p 194.
(44) Nelson, A.; Benton, A. Phospholipid monolayers at the mercury water interface. *J. Electroanal. Chem.* **1986**, *202*, 253−270.
(45) Leermakers, F. A. M.; Nelson, A. Substrate-induced structural changes in electrode-adsorbed lipid layers—A self-consistent field-theory. *J. Electroanal. Chem.* **1990**, *278*, 73−83.
(46) Nelson, A. Influence of biologically active compounds on the monomolecular gramicidin channel function in phospholipid monolayers. *Langmuir* **1996**, *12*, 2058−2067.
(47) Bizzotto, D.; Nelson, A. Continuing electrochemical studies of phospholipid monolayers of dioleoyl phosphatidyl choline at the mercury−electrolyte interface. *Langmuir* **1998**, *14*, 6269−6273.
(48) Whitehouse, C.; O'Flanagan, R.; Lindholm-Sethson, B.; Movaghar, B.; Nelson, A. Application of electrochemical impedance spectroscopy to the study of dioleoyl phosphatidylcholine monolayers on mercury. *Langmuir* **2004**, *20*, 136−144.
(49) Nelson, A. Electrochemistry of mercury supported phospholipid monolayers and bilayers. *Curr. Opin. Colloid Interface Sci.* **2010**, *15*, 1455−1466.
(50) Rueda, M.; Navarro, I.; Prieto, F.; Nelson, A. Impedance measurements with phospholipid-coated mercury electrodes. *J. Electroanal. Chem.* **1998**, *454*, 155−160.
(51) Rueda, M.; Navarro, I.; Ramirez, G.; Prieto, F.; Prado, C.; Nelson, A. Electrochemical impedance study of Tl^+ reduction through gramicidin channels in self-assembled gramicidin-modified dioleoyl-phosphatidylcholine monolayers on mercury electrodes. *Langmuir* **1999**, *15*, 3672−3678.
(52) Rueda, M.; Navarro, I.; Prado, C.; Silva, C. Impedance study of Tl^+ reduction at gramicidin-modified dioleoylphosphatidylcholine-coated mercury electrodes: Influence of gramicidin concentration and the nature of the supporting electrolyte. *J. Electrochem. Soc.* **2001**, *148*, E139−E147.
(53) Rueda, M.; Prieto, F.; Navarro, I.; Romero, R. Phospholipid and gramicidin−phospholipid-coated mercury electrodes as model systems of partially blocked electrodes. *J. Electroanal. Chem.* **2010**, *649*, 42−47.
(54) Buoninsegni, F. T.; Herrero, R.; Moncelli, M. R. Alkanethiol monolayers and alkanethiol|phospholipid bilayers supported by mercury: An electrochemical characterization. *J. Electroanal. Chem.* **1998**, *452*, 33−42.
(55) Krysinski, P.; Zebrowska, A.; Michota, A.; Bukowska, J.; Becucci, L.; Moncelli, M. R.Tethered mono- and bilayer lipid membranes on Au and Hg. *Langmuir* **2001**, *17*, 3852−3857.
(56) Becucci, L.; Moncelli, M. R.; Herrero, R.; Guidelli, R. Dipole potentials of monolayers of phosphatidylcholine, phosphatidylserine and phosphatidic acid on mercury. *Langmuir* **2000**, *16*, 7694−7700.
(57) Moncelli, M. R.; Becucci, L.; Buoninsegni, F. T.; Guidelli, R. Surface dipole potential at the interface between water and self-assembled monolayers of phosphatidylserine and phosphatidic acid. *Biophys. J.* **1998**, *74*, 2388−2397.
(58) Agak, J. O.; Stoodley, R.; Retter, U.; Bizzotto, D. On the impedance of a lipid-modified Hg|electrolyte interface. *J. Electroanal. Chem.* **2004**, *562*, 135−144.
(59) Stauffer, V.; Stoodley, R.; Agak, J. O.; Bizzotto, D. Adsorption of DPOC onto Hg from the G|S interface and from a liposomal suspension. *J. Electroanal. Chem.* **2001**, *516*, 73−82.
(60) Lipkowski, J. Building biomimetic membrane at a gold electrode surface. *Phys. Chem. Chem. Phys.* **2010**, *12*, 13874−13887.

(61) Bizzotto, D.; Yang, Y.; Shepherd, J. L.; Stoodley, R.; Agak, J.; Stauffer, V.; Lathuilliere, M.; Akhtar, A. S.; Chung, E. Electrochemical and spectroelectrochemical characterization of lipid organization in an electric field. *J. Electroanal. Chem.* **2004**, *574*, 167−184.
(62) Elsen, A.; Murphy, B. M.; Ocko, B. M.; Tamam, L.; Deutsch, M.; Kuzmenko, I.; Magnussen, O. M. Surface layering at the mercury−electrolyte interface. *Phys. Rev. Lett.* **2010**, *104*, 105501.
(63) Hauser, H.; Pascher, I.; Pearson, R. H.; Sundell, S. Preferred conformation and molecular packing of phosphatidylethanolamine and phosphatidylcholine. *Biochim. Biophys. Acta* **1981**, *650*, 21−51.
(64) Casal, H.; Mantsch, H. H. Polymorphic phase behaviour of phospholipid membranes studied by infrared spectroscopy. *Biochim. Biophys. Acta* **1984**, *779*, 381−401.
(65) Richer, J.; Lipkowski, J. Measurement of physical adsorption of neutral organic species at solid electrodes. *J. Electrochem. Soc.* **1986**, *133*, 121−128.
(66) Helm, C. A.; Tippmann-Krayer, P.; Möhwald, H.; Als-Nielsen, J.; Kjaer, K. Phases of phosphatidyl ethanolamine monolayers studied by synchrotron X-ray-scattering. *Biophys. J.* **1991**, *60*, 1457−1476.
(67) Jackson, R.; Zamlynny, V. Optimization of electrochemical infrared reflection absorption spectroscopy using Fresnel equations. *Electrochim. Acta* **2008**, *53*, 6768−6777.
(68) Zamlynny, V.; Lipkowski, J. In *Diffraction and Spectroscopic Methods in Electrochemistry*; Alkire, R. C., Kolb, D. M., Lipkowski, J., Ross, P. N., Eds.; Wiley-VCH: New York, 2006; Chapter 9.
(69) *Fresnel 1* software written by V. Zamlynny. E-mail: Vlad.Zamlynny@AcadiaU.ca.
(70) Barner, B. J.; Green, M. J.; Saez, E. I.; Corn, R. M. Polarization modulation Fourier-transform infrared reflectance measurements of thin-films and monolayers at metal-surfaces utilizing real-time sampling electronics. *Anal. Chem.* **1991**, *63*, 55−60.
(71) Green, M. J.; Barner, B. J.; Corn, R. M. Real-time sampling electronics for double modulation experiments with Fourier-transform infrared spectrometers. *Rev. Sci. Instrum.* **1991**, *62*, 1426−1430.
(72) Buffeteau, T.; Desbat, B.; Blaudez, D.; Turlet, J. M. Calibration procedure to derive IRRAS spectra from PM-IRRAS spectra. *Appl. Spectrosc.* **2000**, *54*, 1646−1650.
(73) Zamlynny, V.; Zawisza, I.; Lipkowski, J. PM FTIRRAS studies of potential-controlled transformations of a monolayer and a bilayer of 4-pentadecylpyridine, a model surfactant, adsorbed on a Au(111) electrode surface. *Langmuir* **2003**, *19*, 132−145.
(74) Damaskin, B. B.; Petrii, O. A.; Batrakov, V. V. *Adsorption of Organic Compounds on Electrodes*; Nauka: Moscow, 1968.
(75) Lipkowski, J. Stolberg, L. In *Adsorption of Molecules at Metal Electrodes*; Lipkowski, J., Ross, P. N., Eds.; VCH: New York, 1992; pp 171−238.
(76) Lewis, R. N. A. H.; McElhaney, R. N. Calorimetric and spectroscopic studies of the polymorphic phase behavior of a homologous series of n-saturated 1,2-diacyl phosphatidylethanolamines. *Biophys. J.* **1993**, *64*, 1081−1096.
(77) Casal, H. L.; Mantsch, H. H. The thermotropic phase behavior of *N*-methylated dipalmitoylphosphatidylethanolamines. *Biochim. Biophys. Acta* **1983**, *735*, 387−396.
(78) Mantsch, H. H.; Hsi, S. C.; Butler, K. W.; Cameron, D. G. Studies on the thermotropic behavior of aqueous phosphatidylethanolamines. *Biochim. Biophys. Acta* **1983**, *728*, 325−330.
(79) Cameron, D. G.; Casal, H. L.; Mantsch, H. H. Characterization of the pretransition in 1,2-dipalmitoyl-*sn*-glycero-3-phosphocholine by Fourier transform infrared spectroscopy. *Biochemistry* **1980**, *19*, 3665−72.
(80) Snyder, R. G.; Liang, G. L.; Strauss, H. L.; Mendelsohn, R. IR spectroscopic study of the structure and phase behavior of long-chain diacylphosphatidylcholines in the gel state. *Biophys. J.* **1996**, *71*, 3186−3198.
(81) Umemura, J.; Cameron, D. G.; Mantsch, H. H. A Fourier-transform infrared spectroscopic study of the molecular interaction of cholesterol with 1,2-dipalmitoyl-*sn*-glycero-3-phosphocholine. *Biochim. Biophys. Acta* **1980**, *602*, 32−44.
(82) Mantsch, H. H.; McElhaney, R. M. Phospholipid phase transitions in model and biological membranes as studied by infrared spectroscopy. *Chem. Phys. Lipids* **1991**, *57*, 213−226.
(83) Okamura, E.; Umemura, J.; Takenaka, T. Fourier-transform infrared-attenuated total reflection spectra of dipalmitoylphosphatidylcholine monomolecular films. *Biochim. Biophys. Acta* **1985**, *812*, 139−146.
(84) Mantsch, H. H.; Martin, A.; Cameron, D. G. Characterization by infrared spectroscopy of the bilayer to nonbilayer phase transition of phosphatidylethanolaines. *Biochemistry* **1981**, *20*, 3138−3145.
(85) Snyder, R. G.; Hsu, S. L.; Krimm, S. Vibrational-spectra in C−H stretching region and structure of polymethylene chain. *Spectrochim. Acta A* **1978**, *34*, 395−406.
(86) Chen, C. H. Interactions of lipid vesicles with solvent in heavy and light water. *J. Phys. Chem.* **1982**, *86*, 3559−3562.
(87) Moskovits, M. Surface selection-rules. *J. Chem. Phys.* **1982**, *77*, 4408−4416.
(88) Allara, D. L.; Nuzzo, R. G. Spontaneously organized molecular assemblies. 2. Quantitative infrared spectroscopic determination of equilibrium structures of solution-adsorbed *n*-alkanoic acids on an oxidized aluminium surface. *Langmuir* **1985**, *1*, 52−66.
(89) Allara, D. L.; Swalen, J. D. An infrared reflection spectroscopy study of oriented cadmium arachidate monolayer films on evaporated silver. *J. Phys. Chem.* **1982**, *86*, 2700−2704.
(90) Umemura, J.; Kamata, T.; Kawai, T.; Takenaka, T. Quantitative evaluation of molecular orientation in thin Langmuir−Blodgett films by FT-IR transmission and reflection−absorption spectroscopy. *J. Phys. Chem.* **1990**, *94*, 62−67.
(91) Petty, M. C. *Langmuir−Blodgett Films: An Introduction*; Cambridge University Press: New York, 1996; Chapter 5.
(92) Fringeli, U. P. Structure of lipids and proteins studied by attenuated total reflection (ATR) infrared spectroscopy. 2. Oriented layers of a homologous series−Phosphatidylethanolamine to phosphatidylcholine. *Z. Naturforsch. C* **1977**, *32c*, 20−45.
(93) Yan, W.; Strauss, H. L.; Snyder, R. G. Conformation of the acyl chains in diacylphospholipid gels by IR spectroscopy. *J. Phys. Chem. B* **2000**, *104*, 4229−4238.
(94) Ishioka, T.; Yan, W.; Strauss, H. L.; Snyder, R. G. Normal mode analyses of methyl palmitate all-trans and disordered forms in wagging progressive region. *Spectrochim. Acta A* **2003**, *59*, 671−680.
(95) Madrid, E.; Wilkie, J. Horswell, S. L. Manuscript in preparation.
(96) Wong, P. T. T.; Mantsch, H. H. High-pressure spectroscopic evidence of water binding sites in 1,2-diacyl phospholipids. *Chem. Phys. Lipids* **1988**, *46*, 213−224.
(97) Sen, A.; Yang, P. W.; Mantsch, H. H.; Hui, S.-W. Extended hydrogen-bonded structures of phosphatidylethanolamine. *Chem. Phys. Lipids* **1988**, *47*, 109−116.
(98) Pohle, W.; Selle, C. Fourier-transform infrared spectroscopic evidence for a novel lyotropic phase transition occurring in dioleoylphosphatidylethanolamine. *Chem. Phys. Lipids* **1996**, *82*, 191−198.
(99) Bush, S. F.; Adams, R. G.; Levin, I. W. Structural reorganizations in lipid bilayer systems: Effect of hydration and sterol addition on Raman spectra of dipalmitoylphosphatisylcholine multilayers. *Biochemistry* **1980**, *19*, 4429−4436.
(100) Binder, H.; Pohle, W. Structural aspects of lyotropic solvation-induced transitions in phosphatidylcholine and phosphatidylethanolamine assemblies revealed by infrared spectroscopy. *J. Phys. Chem. B* **2000**, *104*, 12039−12048.
(101) Casal, H. L.; Mantsch, H. H.; Paltauf, F.; Hauser, H. Infrared and ^{31}P-NMR studies of the effect of Li^+ and Ca^{2+} on phosphatidylserines. *Biochim. Biophys. Acta* **1987**, *919*, 275−286.
(102) Casal, H. L.; Mantsch, H. H.; Hauser, H. Infrared studies of fully hydrated saturated phosphatidylserine bilayers. Effect of Li^+ and Ca^{2+}. *Biochemistry* **1987**, *26*, 4408−4416.
(103) Fringeli, U. P. A new crystalline phase of L-α-dipalmitoyl phosphatidylcholine monohydrate. *Biophys. J.* **1981**, *34*, 173−187.

(104) Blume, A.; Huebner, W.; Messner, G. Fourier transform infrared spectroscopy of $^{13}C{=}O$-labeled phospholipids. Hydrogen bonding to carbonyl groups. *Biochemistry* **1998**, *27*, 8239−8249.
(105) Lewis, R. N. A. H.; McElhaney, R. N.; Pohle, W.; Mantsch, H. H. Components of the carbonyl stretching band in the infrared spectra of hydrated 1,2-diacylglycerolipid bilayers: A reevaluation. *Biophys. J.* **1994**, *67*, 2367−2375.